Design of a Monolithically Integrated All-Optical Label Swapper for Spectral Amplitude Code Labels Using Cross-Gain Modulation

Christian Habib[1], Pascual Muñoz[1], Lawrence R. Chen[2], and José Capmany[1]

[1] Optical and Quantum Communications Group - iTEAM, Universidad Politécnica de Valencia, Spain
[2] Photonics Systems Group, Electrical & Computer Engineering Department, McGill University, Montréal, QC, Canada
christian.habib@mail.mcgill.ca, pmunoz@gco.upv.es, lawrence.chen@mcgill.ca

Abstract - *We propose a design for an integrated all-optical label-swapper for packet-switched optical networks using Indium Phosphide technology. The proposed topology is a two stage approach that makes use of cross-gain modulation in a semiconductor amplifier used inside a ring laser topology.*

Introduction

Optical packet networks have attracted much attention as a solution for reducing latency and increasing flexibility in next-generation optical networks [1]. One implementation of packet switched optical networks is optical code multi-protocol label switching (OC-MPLS). OC-MPLS makes it possible to process labels in the optical domain, thereby avoiding power-hungry and costly conversions between electrical and optical domains for payload data [2]. Spectral amplitude coding (SAC) is an attractive implementation of OC-MPLS because it promises simple label processing [2, 3]. Using SAC, part of the channel spectrum is allocated to the OC-MPLS label, as shown in Fig. 1a.

A key component in a OC-MPLS network node is the label swapper, which strips the incoming label, attaches a new label, and reinserts it with the payload. Devices using cross-gain modulation (XGM) in ring cavities have previously been demonstrated which have several desirable characteristics for a label swapper; namely, high extinction and contrast ratios [4]. In particular, a proof-of-concept tabletop label-swapper using a two-stage XGM-based fiber-ring laser has been demonstrated [5]. The main drawbacks of this device were cost, size, and low operating frequency due to a lengthy cavity.

Label Swapper Topology and Principle of Operation

The proposed label swapper is shown in Fig. 1b. The device makes use of two cross-gain modulation (XGM) stages to achieve the desired label swap, which is essentially all-optical multi-wavelength conversion. In both cases, the XGM is realized in a semiconductor optical amplifier (SOA). It should be noted that each XGM stage performs a wavelength conversion, while also performing a logical inversion of the signal. As a result, for a dual stage topology, the output has the same polarity as the input signal.

The first stage is used to convert the input label ($\lambda_{in,1}, \lambda_{in,2}$) to an out-of-band intermediate wavelength (λ_{int}). To achieve this, the modulated input label is first injected into a semiconductor optical amplifier (SOA_1) through an arrayed waveguide grating (AWG). Simultaneously, a continuous wave probe beam at λ_{int} is injected into SOA_1 in a counter-propagating configuration relative to the input beam. The counter-propagating configuration of the first stage minimizes the amount of in-band power transmitted to the second

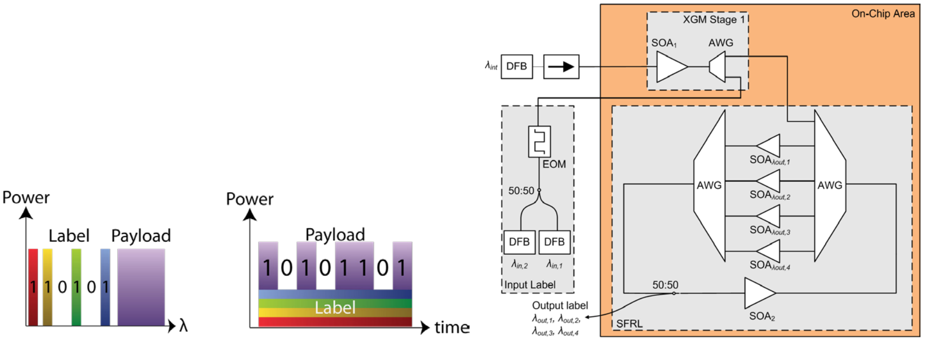

(a) (b)

Figure 1: Fig. 1a Time and wavelength domain representations of an optical packet with SAC-label; Fig. 1b Proposed two stage XGM-based integrated label-swapper.

stage without requiring additional filtering. Note that this stage serves the dual purpose of performing the required logical inversion of the signal (λ_{int} is OFF when the input label is on and vice-versa) as well as ensuring that no power enters the ring laser in the SAC label band (this ensures that output label wavelengths have the same power levels regardless of input wavelength).

The second stage uses XGM in SOA_2 which is placed inside a semiconductor ring laser (SRL). The second stage is biased so it operates slightly above the SRL lasing threshold. When λ_{int} is present, the SRL operates below threshold and no output is produced by the SRL. Conversely, when λ_{int} is absent, the SRL produces power at $\lambda_{out,1},\ldots,\lambda_{out,n}$. Note that λ_{int} is injected via an AWG; it is also removed using an AWG. The output wavelengths are selected using the pass-bands of the AWGs inside the ring. The label swapper can be esily reconfigured to output some or all of the available wavelengths by changing the bias conditions on $SOA_{out,1},\ldots,SOA_{\lambda out,n}$; this compares favorably with the table top demonstrator which used mechanical adjustments (stretching of Fiber Bragg Gratings) [5].

Simulation Details and Results

The topology shown in Fig. 1b was implemented using the VPItransmissionMaker software (version 7.6). The parameters for the devices correspond to the targeted fabrication platform, JePPIX [6–9]. Optimal biasing conditions and device parameters were found and are shown in Tables 1a and 1b. Note that the SRL was assumed to contain 5 mm of waveguides (losses were adjusted accordingly). Furthermore, note that all AWGs were assumed to have Gaussian filtering profiles and 100 GHz channel spacing, with a bandwidth of 40 GHz, and total losses of 6 dB (this includes AWG insertion and transmission losses).

Fig. 2a shows the simulated optical spectrum analyzer traces of the input, intermediate and output wavelengths. Note the clearly visible longitudinal modes that exist within each output label. Their spacing is related to the cavity length, as in [9]. For single-mode ring laser operation, the overall cavity length should be properly adjusted, given the AWG passband bandwidth. Fig. 2b shows the static transfer function of the device as the input

Parameter	*Value*
l_{SOA} (all SOAs)	500 μm
I_{bias} (SOA_1)	178 mA
I_{bias} (SOA_2)	110 mA
I_{bias} $(SOA_{\lambda out,N})$	15 mA
$P_{InputLabel}$ (avg.)	0 dBm
$P_{\lambda,int}$	-21 dBm

(a)

Param.	*Value*
$\lambda_{in,1}$ $\lambda_{in,2}$	1552.52 nm 1551.72 nm
λ_{int}	1554.13nm
$\lambda_{out,1}$ $\lambda_{out,2}$ $\lambda_{out,3}$ $\lambda_{out,4}$	1552.52 nm 1551.72 nm 1550.92 nm 1549.32 nm

(b)

Perf. Metric	*Value*
Static CR	41 dB
OSNR	$>$ 60 dB
$t_{rise/fall}$	295 ps
Dynamic CR	25 dB

(c)

Table 1: Tables 1a & 1b, biasing conditions and device parameters of simulated integrated label swapper; Table 1c, simulated integrated label swapper performance

power level is swept. Fig. 2c shows the input and output temporal traces with a wide bandwidth ($>$ 100 GHz) photodetector module with unit responsivity. Finally, Fig. 2d shows the input and output temporal traces with after conversion to an electrical signal using a photodetector with a bandwidth of 1.25 GHz. Note that the simulation software considers the input laser sources to be temporally coherent, resulting in the beating pattern visible for the input label in Fig. 2c & 2d.

Two static performance metrics are used for the label swapper: (1) the static contrast ratio (SCR), which is defined as the ratio of power in the ON to OFF states for the output label wavelengths, (2) the optical signal-to-noise-ratio (OSNR), which is the ratio of the peak output label wavelength in the ON state to the noise floor.

Full transient simulations were then performed using a PRBS input with a frequency of 1.25 GHz. In particular, we consider the rise and fall times, which are defined as the time required for the output to pass from 10%-90% or 90%-10% of the signal levels. We also consider the dynamic contrast ratio (DCR) which is defined as the ratio of the mean power of ON bits to the mean power of OFF bits for the output label wavelengths. Note that all dynamic results are taken using the photodetector with a 2.5 GHz bandwidth.

Analysis and Conclusion

The results in Table 1c show excellent results in terms of CR and OSNR. In addition, however, it should be noted that the device produces a near-single-mode output for each label wavelength, with better than 25 dB suppression of side modes. In order to compare with our previous results in [5], the power values were determined from the OSA traces using similar resolution bandwidth (60 pm), therefore taking into account the power of all the longitudinal modes within one optical label.

Note that this device requires a wide spacing between label wavelengths due to the use of AWGs; for a transparent optical network, the entire SAC label would need to fit in a single 100 GHz ($\approx$ 0.8 nm) band. AWG performance is limited by lithographic technology. Smaller lithographic features will allow for tighter AWG channel spacing; nonetheless, it may be necessary to investigate other filtering mechanisms to reduce spacing between label wavelength slots. Regarding bidirectional lasing, previous work shows lasing only occurs on one direction [9]. In the simulations, the output label was collected from the counter-clockwise direction as it avoids the need to filter the intermediate wavelength

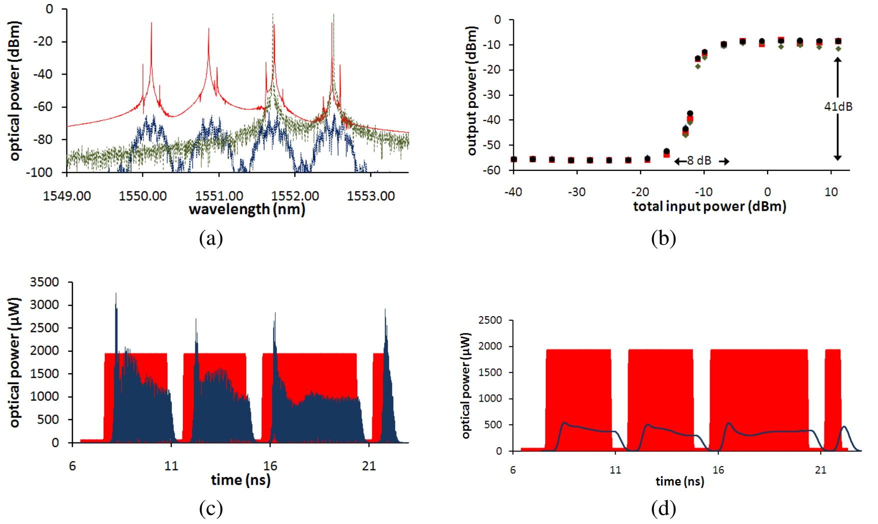

Figure 2: Spectral output, static transfer functions, and dynamic simulations for the label swapper. For 2a, OFF state (blue, dotted), ON state (red, solid), input label (green, dashed). For 2b, $\lambda_{out,1}$ (blue triangles), $\lambda_{out,2}$ (red squares), $\lambda_{out,3}$ (green diamonds), $\lambda_{out,4}$ (black circles). For 2c, the raw output of the label swapper (dark blue) is shown with the input label (red). For 2d the output of the label swapper after a photodetector with limited bandwidth (dark blue) is shown with the input label (red).

from the output signal, but in practice additional filtering should nonetheless be included. In conclusion, the proposed topology shows a marked improvement in frequency response (1.25 GHz), dynamic contrast ratio (25 dB), and reconfiguration speed relative to the previously demonstrated work [5].

References

[1] A. Viswanathan *et al.*, "Evolution of multiprotocol label switching," *IEEE Commun. Mag.*, vol. 36, no. 5, pp. 165–173, May 1998.

[2] N. Wada *et al.*, "Cutting-edge technologies on broadband and scalable photonic network-packet switched networks based on all-optical label processing," *Optical Review*, vol. 11, pp. 106–112, 2004.

[3] P. Seddighian *et al.*, "Low-cost, scalable optical packet switching networks with multi-wavelength labels," in *Proc. OFC/NFOEC '07*. Optical Society of America, 2007, p. OThF5.

[4] R. E. Gordon *et al.*, "Demonstration of all-photonic spectral label-switching for optical MPLS networks," *IEEE Photon. Technol. Lett.*, vol. 18, no. 4, pp. 586–588, Feb. 2006.

[5] C. Habib *et al.*, "All-optical swapping of spectral amplitude code labels using non-linear media and semiconductor fiber ring lasers," *IEEE J. Sel. Topics Quantum Electron.*, (accepted Jan. 2008).

[6] T. DeTemple *et al.*, "On the semiconductor laser logarithmic gain-current density relation," *IEEE J. Quantum Electron.*, vol. 29, no. 5, pp. 1246–1252, May 1993.

[7] T. Durhuus *et al.*, "Detailed dynamic model for semiconductor optical amplifiers and their crosstalk and intermodulation distortion," *J. Lightw. Technol.*, vol. 10, no. 8, pp. 1056–1065, Aug 1992.

[8] M. Hill *et al.*, "Optimizing imbalance and loss in 2 /spl times/ 2 3-db multimode interference couplers via access waveguide width," *J. Lightw. Technol.*, vol. 21, no. 10, pp. 2305–2313, Oct. 2003.

[9] J. den Besten, "Integration of multi-wavelength lasers with fast electro-optic modulators," Ph.D. dissertation, Technische Universiteit Eindhoven, 2004.